Synthesis, Photochromism and Switchable Photoluminescence of a Cd-based Metalloviologen Complex①

SUN Jing[a] YU Cao-Ming[a, b]
CAI Li-Zhen[a②] GUO Guo-Cong[a②]
[a] (*State Key Laboratory of Structural Chemistry, Fujian Institute of Research on the Structure of Matter, Chinese Academy of Sciences, Fuzhou* 350002, *China*)
[b] (*College of Chemical Engineering, Fuzhou University, Fuzhou* 350116, *China*)

ABSTRACT A novel metalloviologen complex $\{[Cd(PhSQ)(HTBC)(H_2O)_2]\cdot 1.25H_2O\}_n$ (**1**) based on N-(4-sulfophenyl)-4,4′-bipyridinium (PhSQ) and monoprotonated trimesic acid (HTBC) has been prepared and structurally characterized. Complex **1** has been characterized by elemental analysis, IR, thermogravimetric analyses, UV-Vis spectra and X-ray crystallography. The coordination geometry of Cd(II) ion is a pentagonal bipyramid. Complex **1** displays a zigzag chain along the *b* axis, and such chains are extended into a 2*D* layer supramolecular network through hydrogen bonding and $\pi\cdots\pi$ interactions. Moreover, complex **1** exhibits reversible photochromic and switchable luminescent behaviors via UV light irradiation at room temperature induced by the photogenerated radicals via a photo-induced electron transfer (PET) mechanism.

Keywords: crystal structure, metalloviologen, photochromism, switchable photoluminescence;
DOI: 10.14102/j.cnki.0254–5861.2011–3101

1 INTRODUCTION

The development of fluorescent materials with modulated emission has recently met with increasing interest due to their potential applications in functional materials[1–3]. Especially, smart luminescent materials which exhibit luminescence on-off switching behaviour are extremely interesting because they can be used to store binary information[4] and prevent tampering or counterfeiting[5–7]. Many approaches utilizing exogenous additives have been focused on tuning fluorescence emission properties, such as thermal-responsive[8, 9], chemical-responsive[10, 11], mechanical-responsive[12, 13], and electrochromic-responsive[14, 15]. However, these stimuli-responsive luminescent materials are not only harmful to environment and humans but also inconvenient for suppliers and consumers without professional chemistry knowledge to handle the anticounterfeiting operation. In contrast, photoresponsive luminescent materials are promising candidates because light has its own advantage due to its noninvasiveness and easy and quick modulation. Moreover, photoswitchable materials can be reversibly interconverted between two discrete states with drastic different optical outputs[16, 17].

Recently, photochromic viologen-functionalized ligands are usually used as functional motif[18] to construct photoswitchable luminescent materials because they can switch the fluorescence resonance energy transfer (FRET) process through photo-induced electron transfer (PIET), and their absorption band of one of the states of the photochromic component has overlap with emission band, making the luminescence quench after the color change via UV light irradiation[19, 20]. We and other groups have found that metalloviologen is easy to assemble and could improve the structural rigidity and radical stability by coordination and intermolecular interactions[21, 22]. In this work, the reactions of a zwitterionic viologen analog, N-(4-sulfophenyl)-4,4′-bipyridinium (PhSQ) with $Cd(NO_3)$ and trimesic acid in water at room temperature gave rise to a new metalloviologen complex $\{[Cd(PhSQ)(HTBC)(H_2O)_2]\cdot 1.25H_2O\}_n$ (**1**), which showed photochromism and realized reversible luminescence modulation between bright and dark states.

Received 18 January 2021; accepted 9 March 2021 (**CCDC 2054226**)
① This research was supported by the program of the Chinese Academy of Sciences (XDB20010100, QYZDB-SSW-SLH020), the NSF of China (21827813, 21871264), and the NSF of Fujian Province (2018J05036, 2018J01028)
② Corresponding authors. E-mails: clz@fjirsm.ac.cn and gcguo@fjirsm.ac.cn

2 EXPERIMENTAL

2. 1 Materials and methods

PhSQ was synthesized according to the literature[23]. Other reagents were purchased commercially and used without further purification. A PLS-SXE300D High Power Xenon Light Source (1.77 W at a distance of 25 cm) was used to prepare colored samples for FT-IR, UV-Vis spectra, powder X-ray diffraction (PXRD), photoluminescence, and electron spin resonance (ESR) studies, and the distances between samples and the Xe lamp were around 25 cm. Elemental analyses were performed on an Elementar Vario MICRO microanalyzer. FT-IR spectra were obtained on a Perkin-Elmer Spectrum One FT-IR spectrometer using KCl pellets in the range of 450～2300 cm^{-1}. Mettler TOLECO simultaneous TGA/DSC apparatus was used to obtain the TGA curve under N_2 atmosphere with a heating rate of 10 K/min. UV-Vis spectra were recorded in an absorbance mode using a PerkinElmer Lambda 950 UV/VIS/NIR spectrophotometer equipped with an integrating sphere, and $BaSO_4$ plates were used as the reference. Powder X-ray diffraction (PXRD) patterns were recorded on a Rigaku MiniFlex II diffractometer using Cu*Kα* radiation. The simulated PXRD pattern was produced by the Mercury Version 2020.1 software using the single-crystal X-ray diffraction data. Electron spin resonance spectra were recorded using a Bruker-BioSpin E500 ESR spectrometer under a 100 kHz magnetic field in the X band (with a microwave frequency of 9.85 GHz) at room temperature. *In situ* determination of photoluminescence was conducted on a double excitation monochromator Edinburgh FL920 fluorescence spectrometer equipped with a R928P PMT detector.

2. 2 Synthesis of the title complex

Compound **1** was prepared by the hydrothermal reaction of $Cd(NO_3)_2$ $4H_2O$ (61.6 mg, 0.2 mmol), PhSQ $3H_2O$ (37.0 mg, 0.1 mmol), trimesic acid (21.0 mg, 0.1 mmol), 5 mL H_2O, and 5 drops of **1** M NaOH solution at 100 ℃ for 3 days. Upon cooling to room temperature, yellow prism crystals of **1** were obtained after filtration. Elemental Analysis (%) calcd.: C, 43.39; H, 3.25; N, 4.05. Found (%): C, 43.37; H, 3.27; N, 4.02.

2. 3 X-ray structure determination

Single-crystal X-ray diffraction measurements were performed on a Rigaku FRX diffractometer equipped with a graphite-monochromated Mo*Kα* radiation (λ = 0.71073 Å) with an ω-scan mode. The intensity data were corrected for *Lp* effects, and empirical absorption corrections were applied using the multi-scan method in the CrysAlisPro software[24]. All structures were solved by direct methods and refined through a full-matrix least-square technique on F^2 using the Siemens SHELXTL package[25]. Hydrogen atoms of the frameworks were added geometrically and refined using the riding model. All non-hydrogen atoms were refined anisotropically. Crystal data for **1** (M_r = 691.41 g/mol): monoclinic system, space group *C*2/*c*, a = 19.0913(5), b = 10.0190(3), c = 27.6160(8) Å, β = 98.597(3)°, V = 5222.9(3) $Å^3$, Z = 8, T = 301(2) K, μ(Mo*Kα*) = 0.988 mm^{-1}, D_c = 1.759 g/cm^3, 12203 reflections measured (2.15°≤ θ ≤ 29.41°), 5025 unique (R_{int} = 0.0276, R_{sigma} = 0.0396) which were used in all calculations. The final R = 0.0278 ($I > 2\sigma(I)$) and wR = 0.0753 (all data). The selected bond lengths and bond angles for **1** are given in Table 1.

Table 1. Selected Bond Lengths (Å) and Bond Angles (°)

Bond	Dist.	Bond	Dist.	Bond	Dist.
Cd(1)–O(7)#1	2.3348(12)	Cd(1)–O(6)#1	2.4678(12)	Cd(1)–N(1)	2.2992(14)
Cd(1)–O(9)	2.2632(11)	Cd(1)–O(4W)	2.3365(13)		
Cd(1)–O(8)	2.5983(12)	Cd(1)–N(1)	2.2992(14)		
Angle	(°)	Angle	(°)	Angle	(°)
O(7)#1–Cd(1)–O(8)	131.45(4)	O(9)–Cd(1)–O(7)#1	78.44(4)	N(1)–Cd(1)–O(7)#1	140.75(4)
O(7)#1–Cd(1)–O(6)#1	54.18(4)	O(9)–Cd(1)–O(8)	53.24(4)	N(1)–Cd(1)–O(8)	87.79(4)
O(7)#1–Cd(1)–O(4W)	89.67(5)	O(9)–Cd(1)–O(6)#1	132.59(4)	N(1)–Cd(1)–O(6)#1	86.61(4)
O(6)#1–Cd(1)–O(8)	173.75(4)	O(9)–Cd(1)–O(4W)	87.90(5)	N(1)–Cd(1)–O(4W)	94.44(5)
O(4W)–Cd(1)–O(8)	84.65(4)	O(9)–Cd(1)–N(1)	140.63(4)	N(1)–Cd(1)–O(3W)	82.69(5)
O(4W)–Cd(1)–O(6)#1	93.03(5)	O(9)–Cd(1)–O(3W)	90.61(5)	O(3W)–Cd(1)–O(7)#1	96.27(5)
O(3W)–Cd(1)–O(4W)	173.46(5)	O(3W)–Cd(1)–O(6)#1	92.67(5)	O(3W)–Cd(1)–O(8)	89.35(5)

Symmetry transformation: #1: *x*, –1+*y*, *z*; #2: *x*, 1+*y*, *z*

3 RESULTS AND DISCUSSION

3. 1 Description of the crystal structure

Compound **1** crystallizes in space group *C*2/*c*. The asymmetric unit contains one Cd atom, two coordinated water molecules, one HTBC ligand, one PhSQ ligand and two lattice water molecules, one of which has the site occupancy of 0.25. The Cd atom is coordinated by two O atoms from two coordinated water molecules, four O atoms from different carboxyl groups of two $HTBC^{2-}$ ligands, and one N atom from the PhSQ ligand to form a distorted pentagonal bipyramid (Fig. 1a). Bond lengths of Cd–O vary from 2.2632(11) to 2.5983(12) Å, and that of Cd–N is 2.2992(14) Å. The Cd^{2+} ions are bridged by $HTBC^{2-}$ ligands to form a zigzag chain along the *b* axis, and each PhSQ ligand is suspended along the *a* axis on the same side of the chain by terminal coordination of N atom with the Cd^{2+} ion, forming a fence-like structure (Fig. 1b). Such chains are extended into a 2*D* layer supramolecular network in *bc*-plane through hydrogen bonding and $\pi\cdots\pi$ interactions (Fig. 1c). As shown in Fig. 1c, strong $\pi\cdots\pi$ interaction can be observed between the adjacent benzene rings of $HTBC^{2-}$ ligand (center-to-center distance: 3.675 Å) and between the adjacent pyridyl ring of PhSQ (center-to-center distance: 3.859 Å), as well as between the benzene ring of $HTBC^{2-}$ and pyridyl ring of PhSQ (center-to-center distance: 3.719 Å). In addition, all three oxygen atoms form C–H$\cdots$O hydrogen bonding interaction with neighboring pyridine and benzene rings (Fig. 1d). Besides, the dihedral angle between the pyridyl rings is 20.953(65)°. These strong $\pi\cdots\pi$ and C–H$\cdots$O interactions are beneficial for radical stabilization.

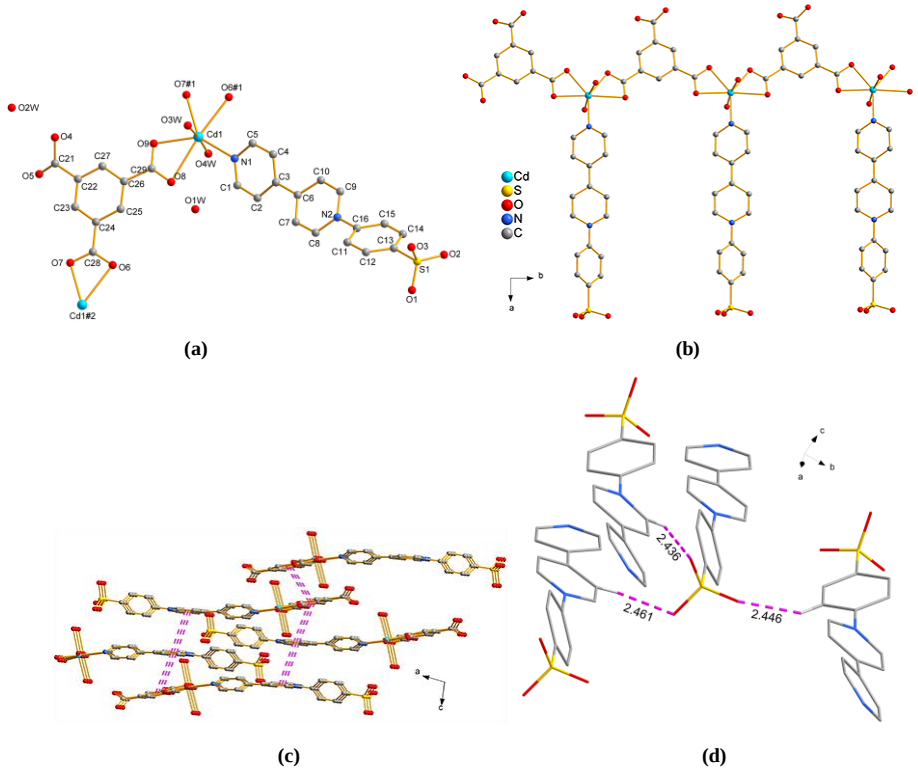

(a) **(b)** **(c)** **(d)**

Fig. 1. Crystal structure of 1: (a) Coordination environments of the Cd^{2+} ion (#1: *x*, –1+*y*, *z*; #2: *x*, 1+*y*, *z*); (b) A zigzag chain; (c) 2*D* layer with $\pi\cdots\pi$ interactions (in angstroms). (d) C–H$\cdots$O interactions; H atoms except the hydrogen-bonding related ones are omitted for clarity

3. 2 Photochromic property

TGA showed that **1** is stable in air below 40 ℃ (Fig. 2a). Then a weight loss of 8.2% from 40 to 190 ℃ with a sharp endothermic peak at 155 ℃ occurred, which was in accordance with the release of 3.25 water molecules (calcd. 8.5%). Complex **1** shows color change from yellow to green upon irradiation of a xenon lamp (Fig. 2b). FT-IR (Fig. 2c) analysis and PXRD (Fig. 2d) indicate no obvious structure change in **1** after irradiation, ruling out the possibility of photoinduced isomerization or photolysis. As shown in Fig. 2e,

three new characteristic electron absorption bands around 420, 640 and 720 nm show up in the absorbance spectra after irradiation and tend to be saturated after irradiation for 40 min, but disappear again after fading 7 days. These bands are similar to those of viologen radicals[26], indicating the formation of PhSQ$^{\bullet}$ free radicals via photoinduced electron transfer. ESR spectra further demonstrate the presence of the photo-generated radical. As shown in Fig. 2f, almost silent signals of the as-synthesized samples were found before irradiation. On the contrast, after irradiation, strong symmetric singlet signals emerged at g = 2.0040 for **1**. These g values are very close to that of a free electron found at 2.0023 in viologen-based complexes[27]. Therefore, the mechanism of photochromic progress could be attributed to photoinduced electron transfer. This progress can be reversed by placing samples in the dark at room temperature.

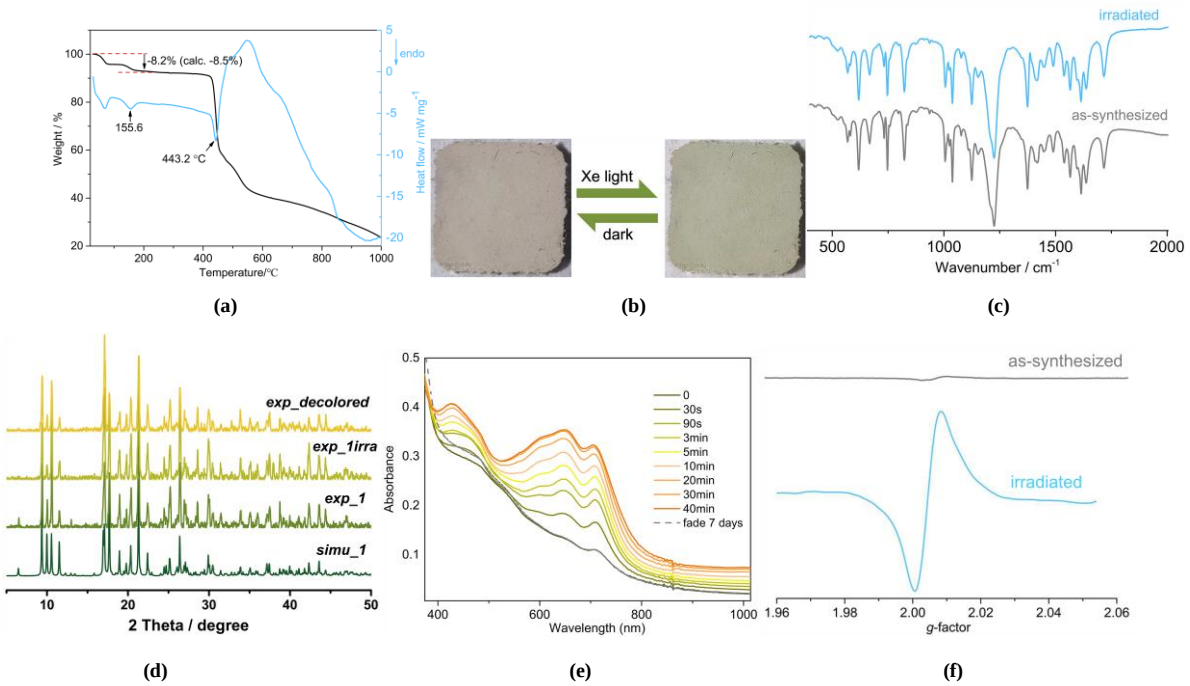

Fig. 2. TGA and DSC curves (a), Color change in the photochromic process (b), FT-IR spectra (c), PXRD patterns (d), Time-dependent absorption spectra upon irradiation (e) and EPR spectra (f) of 1

3. 3 Photoluminescent property

The photomodulated fluorescent property was investigated in solid-state under ambient atmosphere (Fig. 3a). **1** shows emission peak at 420 and 538 nm under excitation of 380 nm. Upon continuous irradiation by using a xenon lamp at room temperature, the emission intensity of **1** decreased gradually with the extension of the irradiation time. After irradiation of 110 minutes, the luminescent intensity at 538 nm decreases to 25% of the initial state, and a slight blue shift of maximum emission peak from 538 to 530 nm appears. The emission peaks of the initial samples of **1** show good overlaps with the photochromic absorption bands of their colored states, so the emission band around 538 nm is absorbed by the colored sample which possesses broad bands in the 400～800 nm range. The weakening of the fluorescence might be attributed to the intramolecular energy transfer from the excitation states to the colored state of the ligands under irradiation of the xenon lamp[28]. In order to understand the photoluminescent mechanism, the photomodulated fluorescent property of PhSQ was also investigated at room temperature. As shown in Fig. 3b, PhSQ shows emission peak at 420 nm with a shoulder peak at 538 nm under 380 nm excitation. The emission intensity of PhSQ showed similar gradual decrease upon continuous irradiation. Therefore, the photoluminescent mechanism of **1** may be assigned to π-π* transitions of the ligand. The enhanced intensity at 538 nm is perhaps attributed to the more rigidity of the ligand coordinated to Cd^{2+} ion that effectively reduces the loss of energy[29–31].

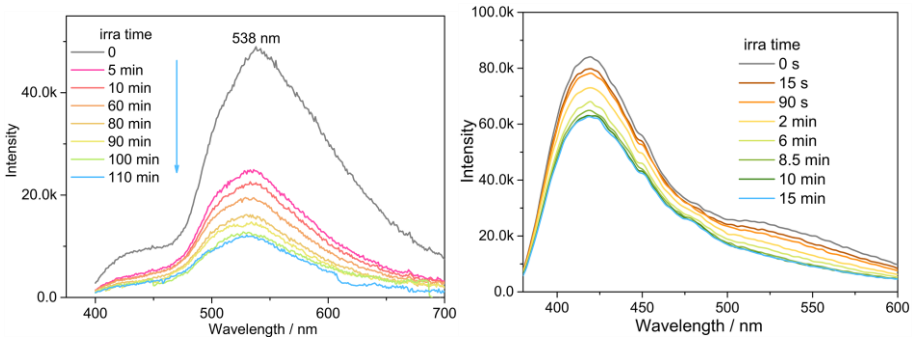

(a) **(b)**

Fig. 3. Luminescence spectra of compound 1 (a) and PhSQ (b) after irradiation with a xenon lamp for different periods of time at room temperature

4 CONCLUSION

In summary, a novel Cd-based metalloviologen complex **1** was prepared and characterized by spectroscopy as well as by single-crystal X-ray diffraction analysis. **1** contains a fence-like 1*D* chain, and such chains are extended into a 2*D* layer supramolecular network in *bc*-plane through hydrogen bonding and $\pi\cdots\pi$ interactions. Moreover, **1** exhibits reversible photochromic property and its photoluminescent intensity decreases gradually accompanied by photochromism. The tunable fluorescent emission of **1** makes it a potentially useful photoresponsive material.

REFERENCES

(1) Lu, Z. S.; Liu, Y. S.; Hu, W. H.; Lou, X. W.; Li, C. M. Rewritable multicolor fluorescent patterns for multistate memory devices with high data storage capacity. *Chem. Commun.* **2011**, 47, 9609–9611.

(2) Bisoyi, H. K.; Li, Q. Light-driven liquid crystalline materials: from photo-induced phase transitions and property modulations to applications. *Chem. Rev.* **2016**, 116, 15089–15166.

(3) Yang, J.; Ren, Z.; Chen, B.; Fang, M.; Zhao, Z.; Tang, B. Z.; Peng, Q.; Li, Z. Three polymorphs of one luminogen: how the molecular packing affects the RTP and AIE properties? *J. Mater. Chem. C* **2017**, 5, 9242–9246.

(4) Sun, J. K.; Cai, L. X.; Chen, Y. J.; Li, Z. H.; Zhang, J. Reversible luminescence switch in a photochromic metal-organic framework. *Chem. Commun.* **2011**, 47, 6870–6872.

(5) Bradberry, S. J.; Savyasachi, A. J.; Martinez-Calvo, M.; Gunnlaugsson, T. Development of responsive visibly and NIR luminescent and supramolecular coordination self-assemblies using lanthanide ion directed synthesis. *Coord. Chem. Rev.* **2014**, 273, 226–241.

(6) Tsang, M. K.; Bai, G.; Hao, J. Stimuli responsive upconversion luminescence nanomaterials and films for various applications. *Chem. Soc. Rev.* **2015**, 44, 1585–1607.

(7) McConnell, A. J.; Wood, C. S.; Neelakan-dan, P. P.; Nitschke, J. R. Stimuli-responsive metal-ligand assemblies. *Chem. Rev.* **2015**, 115, 7729–7793.

(8) Jiang, K.; Wang, Y.; Cai, C.; Lin, H. Conversion of carbon dots from fluorescence to ultralong room-temperature phosphorescence by heating for security applications. *Adv. Mater.* **2018**, 30, 1800783.

(9) Yu, J.; Cui, Y.; Wu, C. D.; Yang, Y.; Chen, B.; Qian, G. Two-photon responsive metal-organic framework. *J. Am. Chem. Soc.* **2015**, 137, 4026–4029.

(10) Li, X.; Xie, Y.; Song, B.; Zhang, H. L.; Chen, H.; Cai, H.; Liu, W.; Tang, Y. A Stimuli-responsive smart lanthanide nanocomposite for multidimensional optical recording and encryption. *Angew. Chem. Int. Ed.* **2017**, 56, 2689–2693.

(11) Hai, J.; Li, T.; Su, J.; Liu, W.; Ju, Y.; Wang, B.; Hou, Y. Reversible response of luminescent terbium(III)-nanocellulose hydrogels to anions for latent fingerprint detection and encryption. *Angew. Chem. Int. Ed.* **2018**, 57, 6786–6790.

(12) Sun, H.; Liu, S.; Lin, W.; Zhang, K. Y.; Lv, W.; Huang, X.; Huo, F.; Yang, H.; Jenkins, G.; Zhao, Q. Smart responsive phosphorescent materials for data recording and security protection. *Nat. Commun.* **2014**, 5, 3601–3609.

(13) Sagara, Y.; Kato, T. Brightly tricolored mechanochromic luminescence from a single-luminophore liquid crystal: reversible writing and erasing of images. *Angew. Chem. Int. Ed.* **2011**, 50, 9128–9132.

(14) Zhang, K. Y.; Chen, X.; Sun, G.; Zhang, T.; Liu, S.; Zhao, Q.; Huang, W. Utilization of electrochromically luminescent transition-metal complexes for erasable information recording and temperature-related information protection. *Adv. Mater.* **2016**, 28, 7137–7142.

(15) Xu, H.; Sun, Q.; An, Z.; Wei, Y.; Liu, X. Electroluminescence from europium(III) complexes. *Coord. Chem. Rev.* **2015**, 293, 228–249.

(16) Wu, H.; Chen, Y.; Liu, Y. Reversibly photoswitchable supramolecular assembly and its application as a photoerasable fluorescent ink. *Adv. Mater.* **2017**, 29, 1605271–5.

(17) Qi, Q.; Li, C.; Liu, X.; Jiang, S.; Xu, Z.; Lee, R.; Zhu, M.; Xu, B.; Tian, W. A solid-state photo-induced luminescence switch for advanced anti-counterfeiting and super-resolution imaging applications. *J. Am. Chem. Soc.* **2017**, 139, 16036–16039.

(18) Guo, G. C.; Yao, Y. G.; Wu, K. C.; Wu, L.; Huang, J. S. Studies on the structure-sensitive functional materials. *Prog. Chem.* **2001**, 13, 151–155.

(19) Xu, G.; Guo, G. C.; Huang, J. S.; Guo, S. P.; Jiang, X. M.; Yang, C. Photochromic inorganic-organic hybrid: a new approach for switchable photoluminescence in the solid state and partial photochromic phenomenon. *Dalton Trans.* **2010**, 39, 8688–8692.

(20) Cusido, J.; Deniz, E.; Raymo, F. M. Fluorescent switches based on photochromic compounds. *Eur. J. Org. Chem.* **2009**, 13, 2031–2045.

(21) Zhang, X.; Wang, M. S.; Sun, C.; Yang, C.; Li, P. X.; Guo, G. C. Stabilizing and color tuning pyrazine radicals by coordination for photochromism. *Chem. Commun.* **2016**, 52, 7947–7949.

(22) Su, Y. B.; Wei, Y. Q.; Cai, L. Z.; Li, P. X.; Wang, M. S.; Guo, G. C. Energy-dependent photochromism at room temperature for visually detecting and distinguishing X-rays. *Chem. Commun.* **2018**, 54, 12349–12352.

(23) Bongard, D.; Moller, M.; Rao, S. N.; Corr, D.; Walder, L. Synthesis of nonsymmetrically N,N′-diaryi-substituted 4,4′-bipyridinium salts with redox-tunable and titanium dioxide (TiO_2)-anchoring properties. *Helv. Chim. Acta* **2005**, 88, 3200–3209.

(24) Sheldrick, G. M. *SADABS: Program for Absorption Correction of Area Detector Frames*. Bruker AXS Inc.: Madison, WI **2001**.

(25) Dolomanov, O. V.; Bourhis, L. J.; Gildea, R. J.; Howard, J. A. K.; Puschmann, H. $OLEX_2$: a complete structure solution, refinement and analysis program. *J. Appl. Crystallogr.* **2009**, 42, 339–341.

(26) Denning, M. S.; Irwin, M.; Goicoechea, J. M. Synthesis and characterization of the 4,4′-bipyridyl dianion and radical monoanion. A structural study. *Inorg. Chem.* **2008**, 47, 6118–6120.

(27) Guo, P. Y.; Sun, C.; Zhang, N. N.; Cai, L. Z.; Wang, M. S.; Guo, G. C. An inorganic-organic hybrid photochromic material with fast response to hard and soft X-rays at room temperature. *Chem. Commun.* **2018**, 54, 4525–4528.

(28) Shi, Q.; Wu, S. Y.; Qiu, X. T.; Sun, Y. Q.; Zheng, S. T. Three viologen-derived Zn-organic materials: photochromism, photomodulated fluorescence, and inkless and erasable prints. *Dalton Trans.* **2019**, 48, 954–963.

(29) Cai, L. Z.; Wang, M. S.; Zhang, M. J.; Wang, G. E.; Guo, G. C.; Huang, J. S. Fluorescent cadmium complexes based on N-succinopyridine ligand: syntheses, structures and tunable photoluminescence by variation of excitation light. *Cryst. Eng. Comm.* **2012**, 14, 6196–6200.

(30) Chen, W. T. Structure and photophysical properties of an upconversion holmium-mercury compound with a 2-*D* layer-like motif. *Chin. J. Struct. Chem.* **2021**, 40, 70–78.

(31) Wang, W. Q.; Chen, J.; Wang, S. H.; Wu, S. F. Synthesis, crystal structure and fluorescence property of a zinc(II) coordination polymer with a theoretical calculation. *Chin. J. Struct. Chem.* **2021**, 40, 79–84.